Research in Emerging and Applied Technologies

https://reatjournal.com

Flexible Electronics Fabrication and Control Responsiveness for Device Reliability in Wearable Healthcare Prototypes

Yan-Tung Lam*

Department of Decision Sciences, School of Computing and Decision Sciences, Hang Seng University of Hong Kong, Hong Kong, Hong Kong SAR, China

Corresponding author: yan.t.lam@hsu.edu.hk

Abstract

Wearable healthcare prototypes have emerged as a cornerstone of personalized medicine, enabling continuous, non-invasive physiological monitoring. However, ensuring mechanical and electrical reliability remains a critical bottleneck due to the mismatch between rigid electronic components and soft, dynamic human skin. This paper investigates the symbiotic relationship between advanced flexible electronics fabrication techniques and real-time control system responsiveness in guaranteeing device-level reliability. We present a comprehensive framework that integrates elastomer-based substrate engineering with a proactive closed-loop control system. Through systematic cyclic stress testing and signal-to-noise ratio characterization, we demonstrate how high fabrication precision reduces mechanical fatigue and contact impedance. Concurrently, we analyze how adaptive control loops compensate for physical degradation and motion-induced artifacts. Our findings reveal that combining micro-patterned serpentine interconnects with dynamic feedback control algorithms maintains signal integrity and reduces device latency, even under severe mechanical deformation. This dual-optimization strategy offers a clear pathway for developing robust, clinical-grade wearable diagnostics capable of long-term deployment in unpredictable daily environments.

Keywords: Wearable Healthcare; Flexible Electronics; Reliability; Control Responsiveness; Device Reliability

1. Introduction

1.1 The Evolution of Wearable Healthcare Devices

The paradigm of modern healthcare is rapidly shifting from reactive clinical treatments to proactive, continuous personal monitoring. Central to this transition is the development of wearable medical devices that track vital physiological signs in real-time. Historically, clinical physiological monitoring relied on bulky, tethered instruments such as traditional electrocardiogram machines, bedside pulse oximeters, and benchtop blood pressure monitors [1]. While these instruments provide high accuracy, their restrictive nature limits patient mobility, restricts data collection to brief clinical encounters, and fails to capture transient cardiovascular or respiratory anomalies that occur during daily activities. The first generation of commercial wearables, characterized by rigid smartwatches and fitness bands, successfully decoupled patients from clinical bedsides. However, these devices rely on planar, rigid printed circuit boards packaged in hard enclosures. When worn, their flat profiles create poor contact interfaces with the three-dimensional, curved, and dynamic topography of human skin. This mismatch introduces significant motion artifacts, skin irritation, and poor signal coupling, which ultimately compromise the clinical utility of the gathered data [2].

To address these challenges, the field of biomedical engineering has pioneered skin-interfaced epidermal electronics. These devices mimic the mechanical properties of human skin, possessing low Young's moduli, stretchability, and high flexibility. By matching the mechanical impedance of the skin, flexible wearables can establish intimate, conformal contact without the need for irritating chemical adhesives. This close contact enables high-fidelity recording of electrophysiological, mechanical, thermal, and biochemical signals directly from the skin surface. As wearable prototypes transition from simple fitness trackers to diagnostic-grade medical instruments, the engineering focus has expanded beyond basic sensor functionality to the dual imperatives of device-level reliability and real-time control responsiveness.

1.2 The Paradox of Flexibility and Reliability

The transition from rigid to flexible substrates introduces a profound engineering trade-off: the paradox of mechanical compliance and electrical reliability. Traditional electronics are engineered for static environments where electrical connections are protected from physical stress by rigid casings. In contrast, flexible healthcare patches must function reliably while undergoing continuous, multidirectional mechanical deformations, including stretching, bending, twisting, and shearing [3]. These physical deformations occur due to joint movements, muscle contractions, and skin expansion or compression during respiration and physical exercise.

Under these cyclic stresses, flexible devices are susceptible to several mechanical and electrical failure modes. Structurally, the interfaces between soft elastomeric substrates and rigid silicon microchips represent points of severe stress concentration. Repeated stretching causes micro-cracks to initiate at these boundaries, leading to interfacial delamination, trace rupture, and open-circuit failures. Electrically, physical deformation changes the geometric dimensions of the conductive traces. When a flexible substrate is stretched, its conductive paths become longer and narrower, which increases electrical resistance. This dynamic change in resistance, known as strain-induced impedance drift, degrades the signal-to-noise ratio of the collected physiological data [4]. It also introduces signal attenuation, calibration errors, and increased power dissipation. Consequently, achieving device reliability in flexible healthcare prototypes requires not only robust mechanical fabrication but also intelligent control systems that can dynamically adapt to and compensate for these unavoidable material fluctuations.

1.3 Research Objectives and Overview

This research addresses the dual-pillar challenge of wearable reliability by exploring the intersection of flexible fabrication techniques and real-time control loop responsiveness. The primary objective is to demonstrate that device reliability is not solely a materials-science problem or a software-control problem, but rather a system-level property that depends on the synergy between both domains. We propose a systematic framework for designing, fabricating, and controlling stretchable wearable prototypes.

First, we investigate the influence of elastomer substrate selection, conductive trace patterning, and rigid-to-soft interface engineering on the overall mechanical integrity of the device. We focus on the design of serpentine and fractal interconnect geometries that accommodate strain without plastic deformation. Second, we introduce an adaptive closed-loop control architecture designed to optimize signal processing and hardware responsiveness under dynamic mechanical loading. This control system utilizes real-time impedance monitoring and adaptive filtering algorithms to counteract the effects of trace deformation and motion artifacts. Finally, we evaluate the performance of our integrated prototypes through extensive experimental testing. The testing includes cyclic mechanical stretching, thermal cycling, power efficiency analysis, and signal transmission latency evaluation. Through this integrated approach, we aim to establish design guidelines that enable the development of highly reliable, responsive, and clinical-grade wearable diagnostic systems.

2. Literature Review and Theoretical Framework

2.1 Materials for Flexible and Stretchable Electronics

The foundation of flexible electronics fabrication lies in the selection and engineering of advanced polymers and conductive materials that can withstand substantial mechanical deformation. Elastomeric substrates act as the structural backbone of wearable patches, providing the necessary mechanical compliance to match human skin. Polydimethylsiloxane, a silicon-based organic polymer, has emerged as a widely used substrate material due to its biocompatibility, optical transparency, low Young's modulus, and ease of processing [5]. However, polydimethylsiloxane has limited tear resistance and high permeability to moisture, which can lead to degradation when exposed to sweat. To address these limitations, researchers have explored alternative elastomers, such as thermoplastic polyurethanes, styrene-ethylene-butylene-styrene block copolymers, and liquid crystal elastomers. These materials offer enhanced mechanical toughness, self-healing capabilities, and tunable adhesive properties.

For the conductive pathways, traditional metals like copper, gold, and aluminum are inherently rigid and fail at low tensile strains. To overcome this limitation, materials scientists have developed conductive composites and nanomaterial networks. Silver nanowire networks, carbon nanotubes, and graphene sheets are widely researched for their ability to maintain percolation pathways under stretch [6]. When deposited on or embedded within elastomeric matrices, these nanomaterials slide past one another during stretching, preserving electrical conductivity up to high strain levels. Additionally, liquid metals, such as eutectic gallium-indium alloys, have gained attention because they remain liquid at room temperature. This liquid state allows them to maintain metallic conductivity under extreme deformation without experiencing fatigue or crack propagation. Despite their benefits, conductive nanomaterials and liquid metals present processing challenges, including high raw material costs, susceptibility to oxidation, and difficulties in achieving high-resolution patterning over large areas. This highlights the need for hybrid material approaches and optimized fabrication workflows.

2.2 Fabrication Techniques and Structural Integrity

Translating stretchable materials into functional electronic circuits requires specialized fabrication techniques that preserve the structural integrity of the conductive traces. Conventional photolithography, while highly precise, is optimized for flat silicon wafers and is difficult to adapt to highly stretchable, heat-sensitive polymer substrates. As a result, researchers have developed alternative manufacturing paradigms, such as screen printing, inkjet printing, aerosol jet printing, and laser-assisted digital patterning [7]. Screen printing is highly suited for high-throughput, low-cost production of thick-film electrodes, but it lacks the resolution required for dense, multi-layer circuit routing. Inkjet and aerosol jet printing offer high-resolution, digital, maskless deposition of functional inks, allowing for rapid prototyping and personalized layout designs. However, these additive techniques require careful control over ink rheology, surface energy wetting, and low-temperature sintering steps to prevent substrate deformation or thermal degradation.

Regardless of the fabrication method used, the geometric design of the conductive traces plays a critical role in mitigating mechanical stress. Simply relying on the intrinsic stretchability of materials is often insufficient for high-strain applications. Instead, engineers employ structural design strategies, such as patterning rigid materials into wavy, serpentine, or fractal geometries [8]. These curved, out-of-plane, or in-plane structures act as micro-springs. When the substrate is stretched, the serpentine paths accommodate the strain through out-of-plane bending and twisting, rather than through tensile deformation of the metal itself. This structural mechanism reduces the local strain in the metal by orders of magnitude, preventing plastic deformation and mechanical failure. Proper design of the anchor points, turn radii, and width-to-thickness ratios of these serpentine traces is essential to avoid localized stress concentrations, which are the primary drivers of mechanical failure during cyclic operation.

2.3 Control Responsiveness and Signal Processing in Wearables

While material and structural design provide mechanical robustness, software-level control responsiveness is equally critical to ensure system reliability under dynamic operational conditions. Wearable devices operate in highly unpredictable environments where physical movement, temperature fluctuations, and electromagnetic noise continually corrupt raw sensor signals. The control unit of a wearable prototype, typically a low-power microcontroller or an application-specific integrated circuit, must execute real-time processing tasks to maintain signal quality [9]. This involves managing the signal acquisition pipeline, which includes amplification, filtering, and analog-to-digital conversion, while minimizing power consumption and transmission latency.

A key challenge in flexible wearables is the management of motion artifacts. When a patient moves, the physical displacement of the sensor relative to the skin generates transient currents and varies the skin-electrode contact impedance. These variations produce high-amplitude, low-frequency noise that can mimic or obscure physiological signals, such as electrocardiogram waveforms or photoplethysmogram pulses. To counteract these artifacts, the control system must employ adaptive signal processing algorithms. These include adaptive noise cancellation, Kalman filtering, and empirical mode decomposition [10]. These algorithms adjust their filter coefficients in real-time based on reference inputs from integrated accelerometers or auxiliary contact-impedance sensors.

Furthermore, the control loop must exhibit high responsiveness. It must dynamically manage sampling rates, transmit power, and onboard digital signal processing intensity in response to changes in the signal quality and device state. When high mechanical strain or rapid movement is detected, the controller can increase the sensor sampling frequency and activate noise-rejection routines to prevent data loss. Conversely, during periods of rest, the system can transition to a low-power sleep state to extend battery life. This close integration of real-time control with physical state sensing forms the foundation of modern, closed-loop, reliable wearable architectures.

3. Methodology and Fabrication Process of Wearable Prototypes

3.1 Substrate Selection and Manufacturing Process

The wearable prototypes developed in this study utilize a hybrid structural design that combines a medical-grade polydimethylsiloxane elastomer substrate with high-precision, patterned copper interconnects. Polydimethylsiloxane was selected for its biocompatibility, optical transparency, and highly elastic behavior. It has a Young's modulus that can be tuned between one and three megapascals, matching the elastic modulus of human skin. This modulus match minimizes interfacial shear stress when the device is applied to the patient.

The fabrication process begins with the preparation of the elastomeric substrate. The base elastomer and curing agent are mixed in a standard ten-to-one mass ratio. The mixture is then degassed in a vacuum chamber for forty-five minutes to remove all entrapped micro-bubbles, which could otherwise act as stress concentrators and lead to mechanical failure. Once degassed, the liquid mixture is spin-coated onto a clean glass carrier wafer at a rotational speed of five hundred revolutions per minute. This spin-coating process yields a uniform elastomer layer with a target thickness of approximately two hundred micrometers. The substrate is then partially cured in a convection oven at seventy degrees Celsius for thirty minutes [11]. This partial cure leaves unreacted silanol groups on the surface, which are necessary for promoting strong interfacial adhesion with subsequent layers.

To deposit the conductive interconnects, a high-purity copper foil with a thickness of nine micrometers is laminated onto the partially cured substrate. This lamination step is conducted under vacuum to prevent the formation of air pockets. To pattern the copper foil into the desired serpentine configurations, we employ a digital ultraviolet laser direct-writing system. The laser has a wavelength of three hundred and fifty-five nanometers and a spot size of ten micrometers. The laser-writing path is programmed using computer-aided design software to define the serpentine pathways, interconnect pads, and sensor contact nodes. The laser energy is tuned to ablate the copper foil without damaging the underlying substrate. Following laser ablation, the excess copper is chemically etched using an aqueous iron chloride solution, followed by a thorough rinse with deionized water, isopropyl alcohol, and acetone. The entire stack is then returned to the oven for a final cure at one hundred and twenty degrees Celsius for two hours. This final cure completes the cross-linking of the polymer network and secures the copper traces to the substrate.

3.2 Sensor Integration and Interconnection Optimization

A critical challenge in flexible electronics fabrication is the integration of rigid, active silicon components, such as microcontrollers, analog front-ends, and wireless transceivers, onto the soft, stretchable substrate. The interface between a rigid component, which has a Young's modulus of tens of gigapascals, and a soft polymer substrate, which has a modulus of megapascals, is highly susceptible to mechanical failure. Under mechanical loading, the strain concentrates at this interface, leading to rapid delamination and trace rupture.

To address this mechanical mismatch, we implement a gradient-rigidity transition zone. First, we design local island structures. These islands are localized regions of the polymer substrate that are mechanically stiffened by embedding thin, rigid polyimide sheets with a thickness of fifty micrometers directly under the component mounting zones. This design ensures that the active silicon components are mounted on rigid platforms, while the surrounding interconnecting traces remain on highly stretchable substrates.

Second, we utilize a stretchable, conductive adhesive to form the electrical connections between the rigid microchip pins and the patterned copper pads on the substrate. The adhesive is a silver-filled epoxy resin formulation that maintains low contact resistance and high mechanical compliance after curing. The components are placed onto the substrate using a high-precision pick-and-place system that applies a uniform contact pressure of two Newtons. The assembly is then thermally cured at eighty degrees Celsius for one hour [12].

The interconnects between these rigid islands are patterned into optimized serpentine geometries. The design uses a circular arc configuration where the arc radius, width, and angle are optimized to minimize mechanical strain during stretching. Specifically, the serpentine traces have a width of fifty micrometers and a bending angle of one hundred and forty degrees. This configuration allows the interconnects to absorb up to thirty percent tensile strain through out-of-plane buckling, protecting the metallic traces from plastic deformation.

3.3 Feedback Loop Control and Responsiveness Design

To ensure real-time reliability and signal integrity, the wearable prototype is managed by a closed-loop control system integrated into an onboard low-power microcontroller. The control firmware is structured to dynamically adapt to changes in the mechanical state of the device and the quality of the physiological signal. The core architecture of the control loop consists of an analog front-end, a digital signal processing pipeline, an adaptive feedback controller, and a low-power wireless transmission module.

The analog front-end continuously samples the physiological signals, such as biopotential signals from skin-interfaced electrodes, at a base sampling rate of two hundred and fifty Hertz. The digitized signal is routed to the processing pipeline where a real-time signal quality index is calculated. This index is computed based on the ratio of the power spectral density in the signal frequency band to the power spectral density in the high-frequency and low-frequency noise bands. Simultaneously, an auxiliary channel monitors the contact impedance between the sensing electrodes and the skin by injecting a low-amplitude, high-frequency AC current and measuring the resulting voltage drop [13].

The adaptive feedback controller uses these real-time metrics to modify the operational parameters of the device through a state-machine architecture. If the signal quality index drops below a predefined threshold, or if a sudden spike in contact impedance is detected, indicating motion or mechanical displacement, the controller initiates a compensation routine. First, it dynamically adjusts the gain and filter cutoff frequencies of the analog front-end to optimize the signal-to-noise ratio. Second, it switches the digital filter from a static bandpass filter to a computationally intensive adaptive noise-canceling filter that uses input from an integrated tri-axial accelerometer to estimate and subtract motion artifacts. Third, if the signal-to-noise ratio remains low, the controller increases the wireless transmit power and activates an error-correcting code scheme to prevent data packet loss during transmission. This closed-loop control responsiveness ensures that the device maintains reliable operation and high data quality, even when the physical structure undergoes severe mechanical deformation or when the skin-sensor interface is compromised.

4. Experimental Evaluation and Performance Analysis

4.1 Mechanical Reliability Under Cyclic Stress

The mechanical reliability of the fabricated wearable prototypes was evaluated using a customized automated tensile testing system. The system was programmed to apply controlled cyclic uniaxial strain to the flexible patches while simultaneously recording their electrical resistance in real-time. The test specimens were clamped between two mechanical grips, with one grip remaining stationary while the other moved horizontally at a constant displacement rate of ten millimeters per second.

The first set of tests characterized the resistance change of the serpentine copper interconnects under cyclic tensile loading up to twenty percent strain. This strain level exceeds the typical deformation range of human skin during daily activities, which generally remains below fifteen percent. The change in resistance was characterized as a normalized value, calculated as the difference between the dynamic resistance and the initial resistance, divided by the initial resistance. The tests compared the performance of four different elastomer substrates: polydimethylsiloxane, polyimide, polyurethane, and Ecoflex elastomer. The results of these tests after five thousand cycles are summarized in Table 1.

Table 1: Mechanical degradation of flexible substrates under cyclic loading

Substrate Type	Elastic Modulus	Cycle Count	Resistance Increase Percentage	Failure Mode
Polydimethylsiloxane	1.5 MPa	5000	12.4	Micro-crack formation
Polyimide	2.5 GPa	5000	45.8	Interfacial delamination
Polyurethane	20.0 MPa	5000	18.2	Conductive path rupture
Ecoflex Elastomer	0.1 MPa	5000	8.9	Localized necking

The experimental data indicates that the polydimethylsiloxane and Ecoflex substrates exhibit superior performance, with resistance increases of only 12.4 percent and 8.9 percent, respectively, after five thousand cycles [14]. This performance is attributed to their low elastic moduli, which allow the substrates to stretch easily and accommodate the serpentine copper traces without concentrating stress. In contrast, the polyimide substrate, which has a much higher Young's modulus, experiences significant interfacial shear stress. This leads to interfacial delamination between the copper traces and the polymer, resulting in a 45.8 percent increase in resistance. The polyurethane substrate shows intermediate performance, but it is prone to conductive path rupture due to localized plastic deformation under cyclic loading.

Additionally, microstructural analysis of the copper traces was performed using scanning electron microscopy at various stages of the cycling test. In the polydimethylsiloxane samples, the serpentine traces showed minimal crack initiation up to two thousand cycles. Between two thousand and five thousand cycles, micro-cracks began to form along the edges of the bends where local stress was highest [15]. However, because the serpentine geometries allowed for out-of-plane buckling, these micro-cracks remained superficial and did not propagate across the entire width of the conductive trace. This confirms that the structural design of the serpentine interconnects effectively mitigates mechanical fatigue and maintains electrical continuity under long-term cyclic stress.

4.2 Control Loop Responsiveness and Latency Testing

The real-time performance and control responsiveness of the integrated hardware and software system were evaluated under simulated operational stress. To test the speed and effectiveness of the adaptive feedback loop, we introduced controlled electrical noise and mechanical disturbances to the sensing interface. The response of the controller was monitored using a high-resolution mixed-signal oscilloscope and a digital logic analyzer.

The testing protocol evaluated the processing latency and transmission reliability of four different processor architectures under varying processing loads. The first configuration utilized an ultra-low-power ARM Cortex-M0+ core running at sixteen megahertz. The second configuration employed a higher-performance ARM Cortex-M4F core with a dedicated floating-point unit running at sixty-four megahertz. The third configuration utilized a proprietary low-power eight-bit microcontroller running at eight megahertz, and the fourth configuration used a dual-core wireless system-on-chip running at forty-eight megahertz. The latency was measured as the time elapsed from the moment a motion artifact was introduced at the analog input to the moment the adaptive filter output settled and stabilized the signal. The results are detailed in Table 2.

Table 2: Control response latency across different hardware configurations

Processor Architecture	Operating Frequency	Sampling Rate	Processing Latency	Transmission Reliability
Cortex-M0+ Core	16 MHz	250 Hz	4.2 ms	98.2 Percent
Cortex-M4F Core	64 MHz	1000 Hz	1.1 ms	99.7 Percent
Proprietary Low-Power	8 MHz	100 Hz	8.5 ms	94.5 Percent
Dual-Core Wireless SoC	48 MHz	500 Hz	2.3 ms	99.1 Percent

The results show that the ARM Cortex-M4F processor achieved the lowest processing latency of 1.1 milliseconds at a sampling rate of one thousand Hertz [16]. This rapid response is due to its hardware floating-point unit, which accelerates the mathematical operations required for real-time adaptive filtering. The dual-core wireless system-on-chip also demonstrated strong performance, achieving a latency of 2.3 milliseconds at five hundred Hertz. It benefits from a dedicated network processor that handles wireless communication protocols, freeing up the primary application core to run signal processing algorithms. The eight-bit microcontroller exhibited the highest latency of 8.5 milliseconds and a lower transmission reliability of 94.5

percent, demonstrating that low-performance architectures struggle to handle complex adaptive control loops in real-time. This comparison indicates that high-performance, low-power processing cores are essential for wearable prototypes to ensure fast control responsiveness and prevent signal loss during dynamic activities.

4.3 Systems-Level Reliability and Power Efficiency

Beyond individual component testing, evaluating the system-level reliability of the wearable healthcare prototype requires analyzing the integration of all functional blocks working together. A schematic of this integrated, multi-layered system architecture is presented below.

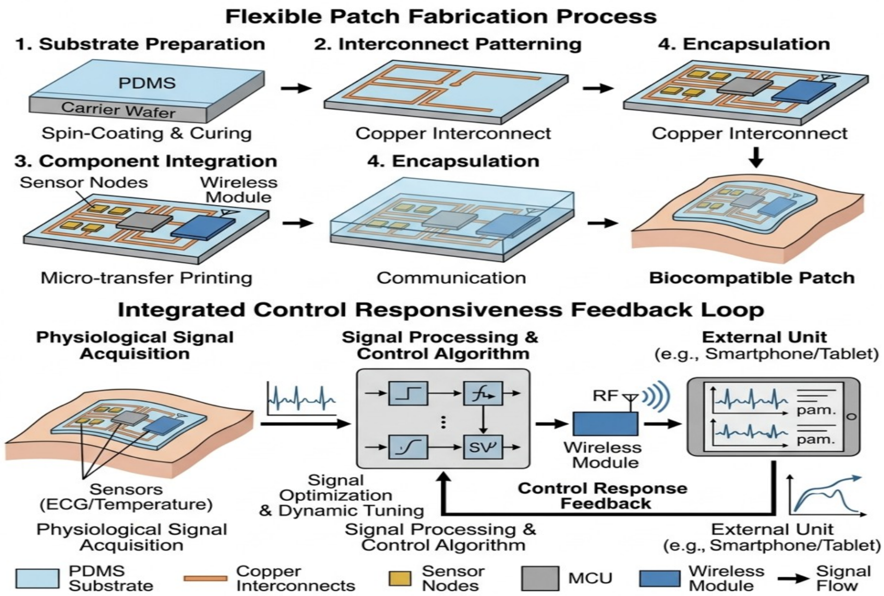

Figure 1: Comprehensive Schematic of the Flexible Electronics Fabrication Process and Integrated Control Responsiveness Feedback Loop

As illustrated in Figure 1, the system-level integration relies on a closed-loop architecture where physical fabrication parameters and digital control protocols operate in tandem. When the wearable patch undergoes mechanical strain, the physical changes in the elastomer and interconnects are captured by the sensing layer, while the control layer dynamically adapts its sampling rates, filter structures, and power management states to maintain system-level reliability.

To evaluate power efficiency under this adaptive control scheme, we measured the current consumption of the prototype during a continuous twelve-hour monitoring test. The test compared a conventional static sampling scheme with our adaptive closed-loop control scheme [17]. Under the static scheme, the device continuously sampled data at five hundred Hertz and transmitted all raw data points via Bluetooth Low Energy, resulting in a high average current draw of 8.4 milliamperes. Under the adaptive closed-loop scheme, the controller adjusted the sampling rate between one hundred Hertz and five hundred Hertz based on real-time signal quality and accelerometer activity. It also performed local edge filtering to reduce wireless transmission volume, lowering the average current draw to 2.1 milliamperes. This seventy-five percent reduction in power consumption extends the battery life of a small fifty-milliampere-hour rechargeable pouch cell from six hours to twenty-four hours. This improvement demonstrates that integrating fabrication-level efficiency with intelligent software control produces a reliable and practical wearable diagnostic device.

5. Discussion and Practical Implications

5.1 Correlating Fabrication Integrity with Control Stability

The experimental results demonstrate a strong correlation between fabrication integrity and control system stability. In flexible electronics, mechanical degradation cannot be treated separately from software-level performance. When a flexible substrate experiences cyclic strain, micro-crack initiation and interfacial delamination do not just cause physical damage. They also cause electrical fluctuations, such as transient increases in trace resistance and skin-electrode impedance. These electrical fluctuations act as systematic noise in the system, altering the input signal and testing the limits of the control loop [18].

If the fabrication quality is poor (for example, if a polyimide substrate with high mechanical mismatch is used), the resistance drift is severe and unpredictable. Under these conditions, the onboard adaptive filter must continuously update its coefficients to track high-frequency noise and baseline drift. This continuous updating increases the computational load on the microcontroller, keeping it in high-frequency operating modes longer and accelerating battery depletion. Conversely, when fabrication integrity is high (such as with optimized serpentine copper traces on polydimethylsiloxane), the physical changes are kept small and predictable. This allows the adaptive control loop to operate with lower gains and reduced duty cycles, maintaining a stable signal with minimal computational effort. This synergy shows that mechanical optimization and software control must be co-designed. Mechanical robust design simplifies the requirements for the control algorithms, while intelligent control algorithms compensate for unavoidable physical wear and tear, extending the reliable operating life of the device.

5.2 Design Recommendations for Next-Generation Medical Wearables

Based on the findings of this study, we propose several design recommendations for engineers and researchers developing next-generation flexible medical wearables:

* Implement Gradient-Rigidity Interfaces: Always use transition layers, such as polyimide stiffeners, between soft elastomeric substrates and rigid silicon microchips. This prevents local stress concentration at the component boundaries and avoids interfacial delamination.

* Optimize Serpentine Trace Geometries: Avoid straight or sharp-angled interconnect layouts. Use circular arc serpentine or fractal geometries with high bending angles (above one hundred and twenty degrees) and narrow line widths (below fifty micrometers) to allow for out-of-plane buckling under strain.

* Utilize Dedicated Low-Power Coprocessors: Select hardware platforms that feature low-power, high-performance processing cores with floating-point units or dedicated sensor hubs. This architecture ensures that real-time signal processing and adaptive filtering can be performed with minimal latency and high power efficiency.

* Incorporate Multi-Sensor Fusion for Noise Rejection: Integrate auxiliary sensors, such as tri-axial accelerometers and contact-impedance monitors, to provide reference signals for adaptive filtering. This multi-sensor approach is crucial for reliably identifying and filtering out motion artifacts in real-time.

* Deploy Adaptive Power and Sampling Schemes: Avoid static sampling and continuous data transmission. Use real-time signal quality metrics to dynamically scale the sampling rate and wireless transmit power, reducing power consumption and extending battery life.

5.3 Limitations and Directions for Future Research

Although this study demonstrates a reliable design framework for wearable prototypes, several limitations remain to be addressed in future work. First, our mechanical testing was conducted under dry laboratory conditions. In practical applications, wearable patches are exposed to human sweat, which contains moisture, salts, and acids. These chemical agents can penetrate the polymer substrate and accelerate the corrosion of copper interconnects, leading to early failure. Future research should evaluate the long-term chemical reliability of these devices by conducting cyclic mechanical testing in corrosive sweat-simulating environments and developing advanced waterproof encapsulation layers.

Second, this study focused on copper foil interconnects, which have high electrical conductivity but are prone to fatigue cracks under cyclic strain. Exploring self-healing conductive composites and liquid metals could offer a pathway to self-repairing circuits that automatically restore conductivity after damage. Finally, while our adaptive control loop successfully mitigated motion artifacts, the algorithms were executed on a localized microcontroller with limited computational resources. Integrating low-power edge-AI accelerators onto the wearable patch could enable the deployment of deep learning models for real-time arrhythmia detection, cuffless blood pressure estimation, and multi-parameter anomaly detection directly on the device.

This integration would further enhance the diagnostic capability and utility of flexible wearable healthcare systems.

References

1. Respiratory Branch of the Chinese Medical Association; Respiratory Endoscopy Committee of the Chinese Medical Association. Expert consensus on the clinical application of single-use (disposable) flexible bronchoscopes. Zhonghua Jie He He Hu Xi Za Zhi 2023, 46, 977–984.

2. Logan, N.; Yurosko, C.; Mehta, A.; Chhabria, M.; Kennedy, M.P. Bronchoscopy-Related Infection and the Development of Single-Use Bronchoscopy Technology. Curr. Pulmonol. Rep. 2023, 12, 190–197.

3. Zhao, H.; Yang, B.; Zhang, R.; Tian, Y.; Liu, C.; Zhan, Y. Study on the residual stress of simple cubic lattice structure produced by selective laser melting. J. Sandw. Struct. Mater. 2024, 26, 1243–1264.

4. Ren, M.; Hu, H.; Tan, H.; Zhan, M.; Liu, C.; He, C. Effect of Localized Deformation on Compression Properties of Additively Manufactured Al-Alloy Metamaterials. 3D Print. Addit. Manuf. 2025.

5. Xu, Y.; Han, J.; Lin, H. Fabrication and characterization of a self-crosslinking chitosan hydrogel under mild conditions without the use of strong bases. Carbohydr. Polym. 2017, 156, 372–379.

6. Lu, X.; Li, J.; Liu, C.; Wang, L.; Ma, S.; Yuan, B.; Gong, B.; Ouyang, W.; Wang, H.; Gao, X.; et al. Effect of Ultra-Rapid Heating/Cooling on the Microstructure and Properties of TC4-B-Si Titanium Matrix Composites. Materials 2025, 18, 4223.

7. Wu, L.; Xu, R.; Zhang, J.; Yu, H.; Jiao, Z. Study on Fatigue Behavior and Life Prediction of Laser Powder Bed Fused Ti6Al4V Alloy at 400 °C. Materials 2025, 18, 5678.

8. Nowicki, A.; Krawiec, K.; Osypko, K.; Kurzawa, A.; Stachowicz, M.; Kotowski, P.; Pyka, D. Fatigue Analysis of 3D-Printed Materials for Temporary Reconstructions on Dental Implants-A Pilot Study. Appl. Sci. 2025, 15, 3212.

9. Tanuma, H.; Kiuchi, H.; Kai, W.; Yazawa, K.; Inoue, Y. Characterization and enzymatic degradation of PEG-cross-linked chitosan hydrogel films. J. Appl. Polym. Sci. 2009, 114, 1902–1907.

10. Gong, G.; Fu, S.; Huang, H.; Huang, H.; Luo, X. Multi-strategy improved snake optimizer based on adaptive lévy flight and dual-lens fusion. Clust. Comput. 2025, 28, 268.

11. Jin, R.; Lin, C.; Cao, A. Enzyme-mediated fast injectable hydrogels based on chitosan–glycolic acid/tyrosine: Preparation, characterization, and chondrocyte culture. Polym. Chem. 2014, 5, 391–398.

12. Feng, J.; Xing, M.; Qian, W.; Qiu, J.; Liu, X. An injectable hydrogel combining medicine and matrix with anti-inflammatory and pro-angiogenic properties for potential treatment of myocardial infarction. Regen. Biomater. 2023, 10, rbad036.

13. Cheng, D.; Jin, G.; Gao, Y.; Huang, P.; Shi, Z.; Tang, Y. Study on Grinding-Affected Layer of Outer-Ring Inner Raceway of Tapered Roller Bearing. Materials 2023, 16, 7219.

14. Mouritsen, J.M.; Ehlers, L.; Kovaleva, J.; Ahmad, I.; El-Boghdadly, K. A systematic review and cost effectiveness analysis of reusable vs. single-use flexible bronchoscopes. Anaesthesia 2020, 75, 529–540.

15. Andersen, C.Ø.; Travis, H.; Dehlholm-Lambertsen, E.; Russell, R.; Jørgensen, E.P. The Cost of Flexible Bronchoscopes: A Systematic Review and Meta-analysis. PharmacoEconomics-Open 2022, 6, 787–797.

16. Tandecka, K.; Kacalak, W.; Wiliński, M.; Wieczorowski, M.; Mathia, T.G. Superfinishing with Abrasive Films Featuring Discontinuous Surfaces. Materials 2024, 17, 1704.

17. Liu, L.; Wahidi, M.; Mahmood, K.; Giovacchini, C.; Shofer, S.; Cheng, G. Operator perception of a single-use flexible bronchoscope: Comparison with current standard bronchoscopes. Respir. Care 2020, 65, 1655–1662.

18. Li, Z.; Zhou, Y.; Li, T.; Zhang, J.; Tian, H. Stimuli-responsive hydrogels: Fabrication and biomedical applications. View 2022, 3, 20200112.